Viser Technology Pte. Ltd.
Mechanical Engineering Science
DOI: 10.33142/mes.v3i1.4334

Research Article Open Access

Wheel Profile Optimization of Speed-up Freight Train Based on Multi-population Genetic Algorithm

Yaodong FU, Dabin CUI*, Pengcheng LEI, Xing ZHANG, Jingkang PENG

School of Mechanical Engineering, Southwest Jiaotong University, Chengdu, China

***Corresponding Author:** Dabin CUI, No.111, North 1st Section, 2nd Ring Road, Chengdu City, 610031, China; cdb1645@163.com*

Abstract:
The geometric shape of the wheel tread is mathematically expressed, and geometric parameters affecting the shape of the wheel were extracted as design variables. The vehicle dynamics simulation model was established based on the vehicle suspension parameters and track conditions of the actual operation, and the comprehensive dynamic parameters of the vehicle were taken as the design objectives. The matching performance of the wheel equivalent conicity with the vehicle and track parameters was discussed, and the best equivalent conicity was determined as the constraint condition of the optimization problem; a numerical calculation program is written to solve the optimization model based on a multi-population genetic algorithm. The results show that the algorithm has a fast calculation speed and good convergence. Compared with the LM profile, the two optimized profiles effectively reduce the wheelset acceleration and improve the lateral stability of the bogie and vehicle stability during straight running. Due to the optimized profile increases the equivalent conicity under larger lateral displacement of the wheelset, the lateral wheel-rail force, derailment coefficient, wheel load reduction rate, and wear index are reduced when the train passes through the curve line. This paper provides a feasible way to ensure the speed-up operation of a freight train.

Keywords: *Speed-up freight trains; Wheel profile optimization; Dynamic performance; Equivalent conicity*

1 Introduction

Railway has always been the main supporting my country's economic development. In 2020, our country's railway freight volume will account for 9.9% of the total social freight volume, and both railway freight volume and freight turnover will rank first in the world[1]; the rapid development of the social economy. At the same time, there are higher requirements for the efficiency of railway transportation, and the most effective way to improve the competitiveness of railway transportation is to increase the speed of freight trains on existing lines. At present, some railway bureaus have proposed optimization of the speed of freight trains for some lines. Plan and implement verification. Under the existing conditions, the speed-up of the vehicle will inevitably increase the force between the wheel and the rail, accelerate wheel-rail wear, reduce the dynamics of the train, and even threaten the safe operation of the vehicle [2-4]. It is very effective to optimize the wheel profile to improve the wheel-rail contact characteristics, improve the dynamic performance of the train, reduce wheel-rail wear, and enhance the production capacity and economic benefits of railway transportation.

Up to now, many achievements have been made in the research of wheel profile optimization design. After analyzing the distribution of tangential and normal forces of the contact model and the influence on wear, Wu [5] took the maximum contact stress, overall wear index, and uniform wheel-rail tread wears as the design objective, based on the existing railhead shape Carry out extended profile design. Cui et al.[6-7] established a weighted normal gap method based on vehicle-track coupling dynamics. According to the given vehicle and track parameters, the weight range of the lateral movement is divided according to the probability of the lateral movement to conveniently optimize the tread surface. Shen et al. [8-9] designed the wheel profile based on the contact angle characteristic curve and the inverse algorithm of the railhead shape combined with software development and applied this method to design a variety of wheel profiles. In Shevtsov et al.[10] wheel profile optimization design method based on the rolling circle radius difference curve, the vertical coordinate of the wheel profile is used as the design variable, the optimal rolling circle radius difference curve is used as the control curve, and the numerical solution of the inverse function problem is used to design the new surface. Jahed et al.[11] uses cubic

Received 25 February 2021; Accepted 28 May 2021

splines to connect the curve segments of the wheel profile in the optimization design method based on the difference of the rolling circle radius to ensure the convexity and concavity and monotony of the wheel profile. Five control parameters are used to improve the design efficiency. Liu [12] used numerical simulation as the main method to study the matching relationship between high-speed wheel and rail profiles in my country. Based on the Chebyshev curve fitting method, he proposed a design method for high-order curve wear-shaped treads, and the wheel wear performance was improved. Cheng et al.[13] proposed a multi-objective profile optimization method based on the response surface of the Gaussian radial basis function. The wheel profile arc parameters were used as the design variables, and the critical speed was used as the objective function. The profile wear index after optimization for the specific vehicle model was improved. Low, better dynamic performance.

Most of the wheel profiles obtained by the above research methods are smooth high-order smooth curves, which can make the wheel-rail contact more smooth and the vehicle dynamics performance is better. However, as the wheel wears, the smooth wheel profile is quickly ground. Roughly, the dynamic performance decreases, and it is difficult to process the wheel profile with discrete high-order curves in actual engineering. This paper takes the wheel profile of freight trains as the research object, establishes the vehicle system dynamics model, and finds the optimal equivalent conicity of the simulated vehicle. The geometric relationship of the wheel tread profile curve is derived, the tread arc parameter is used as the design variable, the dynamic performance of the vehicle is used as the objective function, and the optimal mathematical model of the wheel profile is established, and the model is solved by the multi-population genetic algorithm. The optimized profile was compared and verified with the actual LM profile.

2 Optimal mathematical model

2.1 Design variables

Most standard wheel profiles are arc-shaped wheel profiles, with a definite analytical relationship in geometric expression, and controllable uniformity of wheel-rail contact. By changing the arc parameters of the wheel profile to optimize the wheel profile in engineering applications feasible. Fig.1 shows the geometric expression of the standard wear-type wheel tread. First, the main area in contact with the rail when the vehicle is running determines the optimal area to be 4 arcs between A and E; point A is in phase with the 70° line of the flange tangent, point E is tangent to a straight line segment with a slope of 1:8, B, C, and D are the tangent points of 4 arcs in pairs, O_1~O_4 is the center of each arc, R_1 ~R_4 is the radius of each arc, Z_1 and Z_2 are the contact points with the rail when the wheelset is moved 3mm left and right; Using the wheel-rail geometric contact calculation program of the research group, the coordinates x_{Z1}, y_{Z1}, x_{Z2}, y_{Z2} of Z_1 and Z_2 are obtained from the conical tread surface with the best equivalent conicity of the simulated vehicle. Taking these two points as the fixed points of the optimized profile can make the equivalent conicity of the optimized profile better approximate the best equivalent conicity. Because the tread is in contact with the CN60 rail, R_1 mainly provides the rolling radius difference for the curve with a too-small radius. Keep the fixed value of R_1 unchanged at 14mm. R_4 has less contact with the rail during normal driving and keeps its fixed value unchanged at 220mm, x_D defaults. The distribution intervals of Z_1 and Z_2 points on different wheel profiles are different. For example, LM profiles Z1 and Z2 are distributed in the BC and CD zones respectively, and the LM_A and other profiles are distributed in the CD zone. Therefore, the two cases will be discussed and deduced separately the geometric relationship of the arc parameters in the tread profile in the two cases.

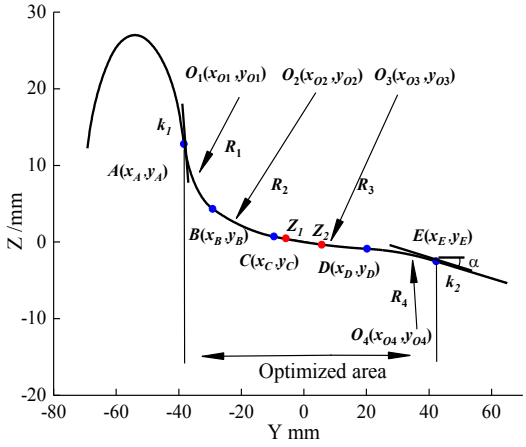

Fig.1 Geometric expression of wheel profile

2.1.1 When Z1 and Z2 are distributed on the arc CD:

If the AB segment is tangent to the -70° straight line segment, its center can be calculated as:

$$\begin{cases} b=y-x\cdot tan(-70^\circ) \\ y_{O1}=tan(-70^\circ)\cdot x_{O1}+b+14\sqrt{1+(tan(-70^\circ))^2} \end{cases} \quad (1)$$

In the formula, y and x are the coordinates of any point on the -70° straight line segment on the wheel flange, and b is the equation constant.

The tangent point A of the arc AB and the -70° straight line segment can be obtained by the following formula:

$$\begin{cases} k_{01}=(-1)/(tan(-70^\circ)) \\ b_{01}=-k_{01}x_{O1}+y_{O1} \\ y_A=tan(-70^\circ)x_A+b \\ y_A=k_{01}x_A+b_{01} \end{cases} \quad (2)$$

In the formula, k_{01}, b_{01} are the slope of the vertical line of the -70° straight line passing the center of the arc AB and the equation constant.

If the arc CD passes through points Z_1 and Z_2, the center O_3 can be calculated by the following formula:

$$\begin{cases} R_3^{\,2} = (x_{O3} - x_{Z1})^2 + (y_{O3} - y_{Z1})^2 \\ R_3^{\,2} = (x_{O3} - x_{Z2})^2 + (y_{O3} - y_{Z2})^2 \end{cases} \tag{3}$$

The arc *BC* is tangent to the arc *AB* and *CD*, and its center O_2can be calculated by the following formula:

$$(x_{O2} - x_{O1})^2 - (y_{O2} - y_{O1})^2 - (R_3\text{-}R_2)^2 + (x_{O3} - x_{O2})^2 + (y_{O3} - y_{O2})^2 = 0 \tag{4}$$

The tangent point of the arc AB and BC is at the intersection of the straight line O_1O_2 and the arc. Point B can be obtained by the following formula:

$$\begin{cases} k_{12} = (y_{O2} - y_{O1}) / (x_{O2} - x_{O1}) \\ b_{12} = -k_{12} x_{O1} + y_{O1} \\ y_{O1} = y_B + \sqrt{R_1^{\,2} - (x_{O2} - x_B)^2} \\ y_B = k_{12} x_B + b_{12} \end{cases} \tag{5}$$

In the formula, k_{12} and b_{12} are the slopes of the straight line O_1O_2 and the equation constant.

The tangent point of the arc BC and CD is at the intersection of the straight line $O_2O_3$and the arc. Point C can be obtained by the following formula:

$$\begin{cases} k_{23} = (y_{O3} - y_{O2}) / (x_{O3} - x_{O2}) \\ b_{23} = -k_{23} x_{O2} + y_{O2} \\ y_{O2} = y_C + \sqrt{R_2^{\,2} - (x_{O2} - x_C)^2} \\ y_C = k_{23} x_C + b_{23} \end{cases} \tag{6}$$

In the formula, k_{23} and b_{23} are the slopes of the straight line O_2O_3 and the equation constant.

The arc CD and DE are tangent at point D, and y_D can be obtained from the following formula:

$$y_D = y_{O3} - \sqrt{R_3^{\,2} - (x_{O3} - x_D)^2} \tag{7}$$

k_{34} is the slope of the straight line O_3O_4 can be obtained by the following formula:

$$k_{34} = (y_{O3} - y_D) / (x_{O3} - x_D) \tag{8}$$

β is the angle between the straight line O_4 and the horizontal line, β can be calculated by k_{34}, and the center O_4 of the arc *DE* can be obtained by the following formula:

$$\begin{cases} \beta = arctan(|\, k_{34} \,|) \\ x_{O4} = x_D - R_4 \cos\beta \\ y_{O4} = y_D - R_4 \sin\beta \end{cases} \tag{9}$$

The arc and the straight line segment with slope k_2 intersect at point E, which can be obtained by the following formula:

$$\begin{cases} \alpha = arctan(|\, k_2 \,|) \\ x_E = x_4 + R_4 \sin\alpha \\ y_E = y_4 + R_4 \cos\alpha \end{cases} \tag{10}$$

At this point, each arc parameter in the optimized area of the wheel profile can be expressed by the arc radius R_2, R_3, and the abscissa x_{o1} of the arc AB's center. These three unknowns are used as the optimization variables of the model:

$$\boldsymbol{v} = [R_2, R_3, x_{O1}] \tag{11}$$

The 4 tangent arcs can be expressed as:

$$C_i = f_i(\boldsymbol{v}) \tag{12}$$

In the formula, $f_i (i = 1,2,3,4)$is the analytical equation of each arc.

Given the four-segment arc equation, the profile curve of the optimized wheel area can be expressed as:

$$C_{\text{wheel}} = f_w(\boldsymbol{v}) \tag{13}$$

In the formula, f_w is the analytical equation of the optimized area profile curve.

2.1.2 When Z1 and Z2 are respectively distributed on the arcs BC and CD:

The arc *CD* passes *C*, Z_2 points, then the circle center O_3 can be calculated by the following formula:

$$\begin{cases} R_3^{\,2} = (x_{O3} - x_C)^2 + (y_{O3} - y_C)^2 \\ R_3^{\,2} = (x_{O3} - x_{Z2})^2 + (y_{O3} - y_{Z2})^2 \end{cases} \tag{14}$$

The arc *BC* passes through Z_1, the point *C* is tangent to the arc *CD*, and its center O_2, R_2 can be calculated by the following formula:

$$\begin{cases} k_{23} = (y_{O3} - y_C) / (x_{O3} - x_C) \\ b_{23} = -k_{23} x_{O3} + y_{O3} \\ k_{22} = -1 / ((y_C - y_{Z1}) / (x_C - x_{Z1})) \\ b_{22} = -k_{22} x_{BB} + y_{BB} \\ y_{O2} = x_{O2} \cdot k_{23} + b_{23} \\ y_{O2} = x_{O2} \cdot k_{22} + b_{22} \\ R_2^{\,2} = (x_{O2} - x_C)^2 + (y_{O2} - y_C)^2 \end{cases} \tag{15}$$

In the formula, k_{23} and b_{23} are the slopes of the straight line O_3C and the equation constants, x_{BB} and y_{BB} are the coordinates of the midpoint of the chord of the arc Z_1C, k_{22} and b_{22} are the slope of the vertical line of the chord of the arc Z_1C, and the equation constants.

The arc of segment *AB* is tangent to the -70° straight line segment, and at the same time tangent to the arc of segment *BC*, its center O_1 can be calculated as:

$$\begin{cases} b = y - x \cdot tan(-70^\circ) \\ y_{O1} = tan(-70^\circ) \cdot x_{O1} + b + 14\sqrt{1 + (tan(-70^\circ))^2} \\ (R_2 - 14)^2 = (x_{O2} - x_{O1})^2 + (y_{O2} - y_{O1})^2 \end{cases} \tag{16}$$

In the formula, y and x are the coordinates of any point on the -70° straight line segment on the wheel flange, and b is the equation constant.

The geometric derivation formulas of the remaining arc parameters and the first distribution will not be repeated. At this point, each arc parameter in the wheel profile optimization area can be expressed by the arc radius R_3 and the coordinate of point C, x_C, y_C These three unknowns are used as the optimization variables of the model:

$$\boldsymbol{v} = [R_3, x_C, y_C] \tag{17}$$

The 4 tangent arcs can be expressed as:

$$C_i = f_i(\boldsymbol{v}) \tag{18}$$

In the formula, $f_i (i = 1,2,3,4)$ is the analytical

equation of each arc.

Then the profile curve of the optimized wheel area can be expressed as:

$$C_{\text{wheel}} = f_w(\boldsymbol{v}) \tag{19}$$

In the formula, f_w is the analytical equation for optimizing the area profile curve.

2.2 Objective function

Taking the comprehensive dynamic performance index of freight trains as the objective of surface optimization design, the vehicles run at speed on existing lines, and the track irregularity of my country's mainline railway is between the fifth and sixth class railways in the United States [15]. Setting the American five-level spectrum as the line irregularity incentive. Although the straight-line accounts for a higher proportion of the total line length, refer to the actual operation situation. Because the dynamic performance of the vehicle rarely exceeds the standard when the vehicle is running in a straight line, the exceeding often occurs in the curve operation, so the simulation condition is set as: the length of the straight line is 600 m, the sampling frequency is 200 Hz, and the speed is 90km/h. The curve selects the smallest radius curve that allows vehicles to pass 90km/h. The line parameters are shown in Table 1.

Table 1. Simulation parameters of small radius curve

Serial number	parameter name	Numerical value
1	Straight length	600m
2	Easing curve length	100m
3	Curve radius	R800m
4	Circular curve length	500m
5	Super high line	100mm
6	Sampling frequency	200Hz
7	Running speed	90km/h

Since the derailment coefficient, wheel load reduction rate, and other indicators are not exceeded during straight-line running, the main concern is the straight-line running stability of the vehicle. Therefore, the RMS value of the lateral acceleration of the wheelset and the body stability is selected to measure the straight-line running performance. When the curve is running, more attention is paid to the running stability of the vehicle, so the derailment coefficient, wheel load reduction rate, and wheel axle lateral force when the train passes a small radius curve is selected to measure the curve passing performance of the train, and the objective function is established as formula (20):

$$\min \begin{cases} f_1(\boldsymbol{v}) = \max(s\ddot{y}) \\ f_2(\boldsymbol{v}) = W \\ f_3(\boldsymbol{v}) = \max(|\,(Q_l / P_l)\,|, |\,(Q_r / P_r)\,|) \\ f_4(\boldsymbol{v}) = \max(\Delta P / P) \\ f_5(\boldsymbol{v}) = \max(|\,Q_r - Q_l\,|) \end{cases} \tag{20}$$

In the formula, f_1 represents the maximum value of the RMS lateral acceleration of the left and right wheelsets during straight running, f_2 represents the train stability index during straight running, f_3 represents the maximum derailment coefficient of the left and right wheels during curve running, and f_4 represents wheel weight reduction during curve running. The maximum load factor, f_5 represents the maximum lateral force of the wheel axle when the curve is running.

Based on the importance of the five objective values and their actual operating performance, it is hoped that both the curve and straight-line performance will be improved. This example sets weighting coefficients respectively for them, among which w_1=0.25, w_2=0.15, w_3=0.2, w_4=0.2, w_5=0.2. At the same time, f_1 to f_5 are normalized with the limit of each kinetic index. The optimization objective function can be expressed as:

$$min\ f\ (\boldsymbol{v}) = w_1 \frac{f_1}{5} + w_2 \frac{f_2}{3.5} + w_3 f_3 + w_4 \frac{f_4}{0.65} + w_5 \frac{f_5}{35} \tag{21}$$

2.3 Constraint equation

The arctangent point should satisfy the following relationship in the optimization area:

$$g_1 = x_E < x_D < x_C < x_B < x_A \tag{22}$$

Considering to ensure that the wheel profile is well matched with the CN60 rail, the wheel profile R_2 and R_3 should meet the following conditions:

$$g_2 = \begin{cases} 85 \le R_2 \le 140 \\ 400 \le R_3 \le 700 \end{cases} \tag{23}$$

When the points Z_1 and Z_2 are distributed on two arcs, the wheel profile R_2 and R_3 should meet the following conditions:

$$g_2 = \begin{cases} y_C < k_z \cdot x_C + b_z \\ 85 \le R_2 \le 140 \\ 400 \le R_3 \le 700 \end{cases} \tag{24}$$

Where k_z and b_z are the slopes of the straight line Z_1Z_2 and the equation constant respectively.

At the same time, to ensure that the equivalent conicity of the optimized profile should meet the best equivalent conicity of the simulated vehicle as much as possible, the equivalent conicity of the optimized profile should meet the following conditions:

$$g_3 = \lambda_{min} < \lambda_e < \lambda_{max} \tag{25}$$

In the formula, λ_e R is the equivalent conicity when the wheelset is laterally moved by 3mm and λ_{min} λ_{max} is determined by the best equivalent conicity of the simulated vehicle.

From equation (20) ~ equation (25), the optimal mathematical model can be expressed as:

$$\begin{cases} f\ (\boldsymbol{v}) \to \min \\ st: g_1, g_2, g_3 \end{cases} \tag{26}$$

3 The optimal equivalent conicity

Based on the measured vehicle parameters of a certain

type of freight train on the East Longhai Line (the main performance parameters are shown in Table 2), CN60 rails are used, the gauge is 1435 mm, the inner distance of the wheelset is 1353 mm, the rail cant is 1/40, and the multi rigid body dynamics software [16-17] establishes the dynamics model of the vehicle system. Fig.2 shows the topology of the vehicle structure.

Table 2 Main vehicle parameters

Serial number	parameter name	Numerical value
1	Vehicle body mass	17500kg
2	Side frame quality	373.5kg
3	Wheelset quality	1154kg
4	Bolt quality	373.5kg
5	Vehicle distance	11.7m
6	Suspension span	1.956m
7	Crossbar stiffness	14.8MN/m
8	Wheelbase	1.75m
9	Wheel radius	0.42m

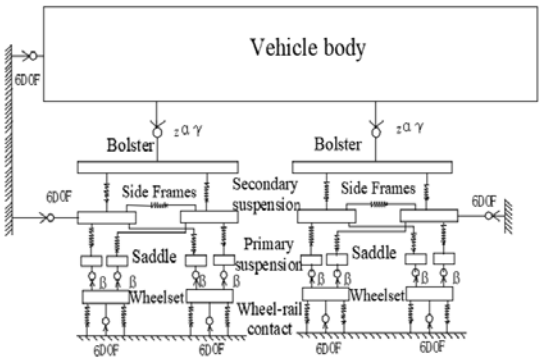

Fig.2 Topological diagram of the vehicle structure

Due to the unevenness of the track, the wheel-rail rolling contact process will form a rolling radius difference that leads to hunting motion [18]. The equivalent conicity can be obtained through a certain algorithm from the rolling circle radius difference. The equivalent conicity of the wheelset is commonly used in engineering to explain its relationship with vehicle dynamics. The straight-line section accounts for more than 80% of freight trains in speed-up operation. The critical speed of train snaking instability is the main evaluation index to measure the stability of the train system's straight-line operation. Based on the definition of equivalent conicity [19], the nominal equivalent conicity (The wheelset lateral displacement 3mm) and the hunting critical speed of the vehicle are studied. The Conical tread is equivalent to the linearization of the main tread, which can ensure that the equivalent conicity varies within a certain range and the equivalent conicity does not change. Based on the shape of the conical tread of TB449-1976 locomotive wheels [20], 13 conical treads with different equivalent conicity between 0.032-0.16 are designed. Fig. 3 only shows the equivalent conicity of the tread with equivalent t conicity of 0.032, 0.05, 0.107, and 0.16.

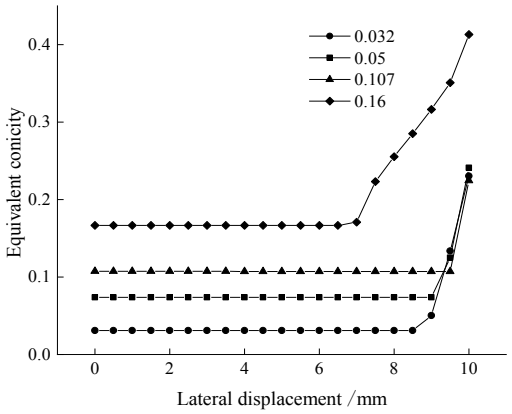

Fig.3 The equivalent conicity of different Conical treads

Using the following method to calculate the critical hunting speed of a freight train can be described as First, let the vehicle pass through an 800m long line with excitation at a certain speed. If the train derails, the speed is higher than the critical speed of the vehicle. Reduce the speed and continue driving. When the vehicle is not derailed, set the vehicle to the same speed at the ideal level. When driving on a straight track, if the wheelset of the vehicle oscillates with a constant amplitude at this time, this speed is defined as the non-linear critical speed of the vehicle. The critical speeds of different treads obtained by simulation calculation using the above-mentioned vehicle model are shown in Fig.4. As the equivalent conicity increases, the critical speed of the vehicle reaches the maximum and then decreases, which is similar to the critical hunting speed distribution proposed by Polach [21]. It is different from the traditional belief that the larger the equivalent conicity, the smaller the critical speed. This is because it is related to vehicle suspension parameters [22], When the equivalent conicity is small, the gravity suspension stiffness of the vehicle will be small, and when the wheelset deviates from a certain distance due to certain excitation, the wheels cannot provide enough guiding force to keep the wheels running along the centerline of the track. Therefore, the optimal tread equivalent conicity of this model should be designed at about 0.107.

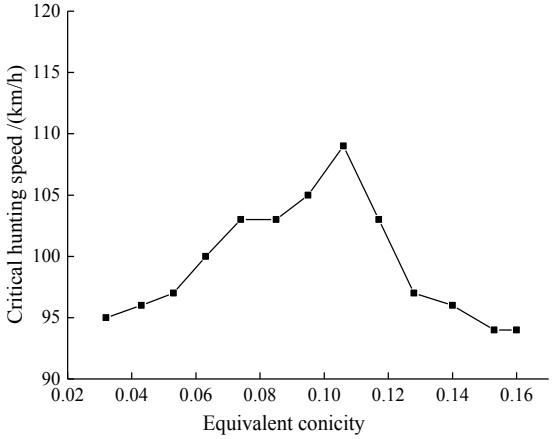

Fig.4 Critical hunting speed of different conical treads

4 Optimization method

4.1 Multi-population genetic algorithm

Multi-population genetic algorithm [23-24] is improved based on genetic algorithm, which solves the premature problem of traditional genetic algorithm. The optimization of traditional genetic algorithms is mainly reflected in the following aspects:

(1) Simultaneous optimization of multiple populations, different populations are given different control parameters to achieve different search purposes.

(2) Coordinated evolution between populations is realized through the connection of migration operators.

(3) Manually select the operator to save the optimal solution of various groups to determine the convergence of the algorithm.

The main content of the multi-population genetic algorithm is: the solution data of the solution space is expressed as the genotype string data of the genetic space through coding, and the string structure data of different combinations constitute different individuals;

Randomly generate an initial population composed of N populations. Each population contains P initial individuals. Start the evolution with the initial population as the starting point. Perform fitness evaluation on each individual and select the outstanding individuals as the parent to breed the next generation of offspring. Through the crossover operation, the new individual can inherit the characteristics of the parent individual, and at the same time, a few individuals are randomly selected to perform mutation operations to change their genes, and the populations are migrated to find the worst individuals of the target population to replace them with the best individuals of the source population, and repeat the evolution finally gets the optimal individual. The main control parameters of the multi-population genetic algorithm include population number (N), population size (P), binary digits of variables (Pr), individual length (D), optimal individual minimum retention algebra (MG), generation gap ($GGAP$), Crossover probability (Pc) and mutation probability (Pm). Among them, N and P represent the abundance of population information, which affects the calculation amount of the algorithm and the optimization speed of the optimization problem; Pr controls the accuracy of the variable; D represents the length of each vector in the population, which is determined by the number of variables; MG affects the optimal solution $GGAP$ determines the ratio of parent generation to be replaced; Pc controls the degree of information exchange between parent and offspring, affecting population diversity and the global search ability of the algorithm, Pm represents the probability of an individual's gene mutation, which affects The local search capability of the algorithm.

4.2 Wheel profile optimization

Before the algorithm starts, set the control parameters in the algorithm, and express the wheel profile variables in the optimization model in the form of population individuals:

$$\boldsymbol{v} \rightarrow \boldsymbol{x} = (d_1, d_2 \cdots d_D) \tag{27}$$

In the formula, $\boldsymbol{x}$ represents the individual vector in the population, and d represents the variables in respectively.

Then the population can be expressed as:

$$\boldsymbol{X} = \begin{cases} [\boldsymbol{x}_{11}; \boldsymbol{x}_{12}; \cdots; \boldsymbol{x}_{1P}] \\ [\boldsymbol{x}_{21}; \boldsymbol{x}_{22}; \cdots; \boldsymbol{x}_{2P}] \\ . \\ . \\ [\boldsymbol{x}_{N1}; \boldsymbol{x}_{N2}; \cdots; \boldsymbol{x}_{NP}] \end{cases} \tag{28}$$

In the formula, $\boldsymbol{X}$ represents the initial population composed of N populations, and each population is composed of P individual vectors.

The specific process is shown in Fig.5: Input the vehicle parameters and track parameters into the vehicle model, and calculate the best equivalent conicity; The initial population $\boldsymbol{X}$ is randomly generated in the constraint space. Each individual in the population corresponds to a wheel profile. The equivalent conicity of each profile is calculated. The individuals that do not meet the equivalent conicity constraints are marked as inferior individuals and their fitness is set as low. The rest of the profiles are imported into the multi-body dynamics software for simulation and the objective function value $f(\boldsymbol{v})$ is calculated, and the optimal profile is selected. When the optimal profile retention algebra is less than the set retention algebra, the fitness $Fv(i)$ of various groups is calculated, and a new population $\boldsymbol{U}$ is obtained by operations such as selection, crossover, mutation, reinsertion, and immigration based on the fitness. Continue to evolve until the optimal profile meets the minimum maintenance algebra, and the optimal wheel profile can be obtained by obtaining the optimization result. The entire solution process is carried out in a closed loop.

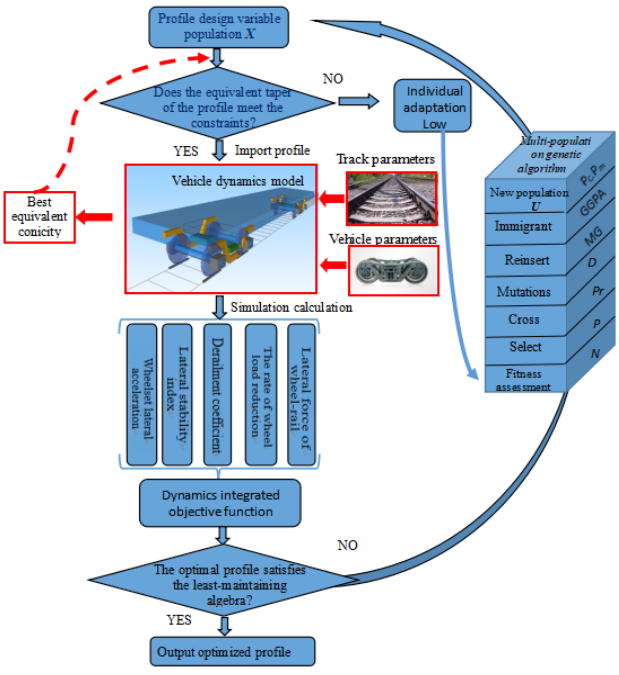

Fig.5 Flow chart of profile optimization

5 Results and analysis

5.1 Optimization Results

By programming and calculating the process shown in Fig.5, the relevant control parameters (Table 3) of a variety of genetic algorithms are selected to design the wheel profile. For the two situations where the wheelset lateral displacement is 3mm contact point pair distribution, The range of design variables is shown in Table 4、Table 5.

Table 3 Calculation parameters

Serial number	parameter name	Numerical value
1	N	5
2	P	20
3	Pr	20
4	D	3
5	MG	20
6	$GGAP$	0.9
7	P_c	(0.7-0.9)
8	P_m	(0.001~0.05)

Table 4 Design variables value

Serial number	parameter name	Numerical value
1	R_2	(85~140)
2	R_3	(400~700)
3	x_{o1}	(-25.1~-25.9)

Table 5 Design variables value

Serial number	parameter name	Numerical value
1	R_3	400~700)
2	x_C	(-8~-10.5)
3	y_C	(0.757~1)

Fig.6 shows the evolution curve of the optimization process of the two optimization profiles. It can be seen that when the number of evolutions reaches 47 and 53, the objective function has achieved the objective optimum respectively. When the optimal solution remains for 20 generations, the algorithm stops. The two optimized profiles stopped after the 66th and 74th generations respectively, which proved that the method has a better convergence speed and obtains the ideal wheel profile faster.

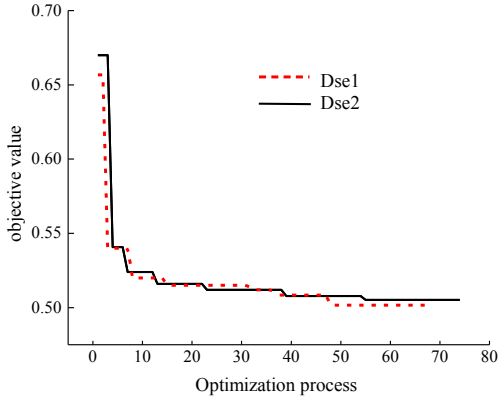

Fig.6 Des1, Des2 optimization process

5.2 Wheel-rail contact state

Fig.7 shows the LM profile and the optimized profile Des1 (the contact point of the wheelset traverses 3mm on the arc CD) and the optimized profile Des2 (the wheelset traverses the 3mm contact point on the arc BC and CD Top) Distribution map of contact point pairs with CN60 rail. It can be seen that when the Des1 profile and Des2 profile have a lateral displacement of 3mm from the left and right of the wheelset, their contact points are more concentrated on the wheel. The width of the distribution range is respectively: LM is 8.83mm, Des1 is 7.1mm, and Des2 is 8.5mm. When the two optimized profiles are running in a straight line, the change range of the contact position of the wheel tread is smaller, and the vehicle will travel more smoothly. When the wheelset lateral displacement is large, the matching characteristics at the flange of the wheel remain unchanged due to the same parameters of the wheels.

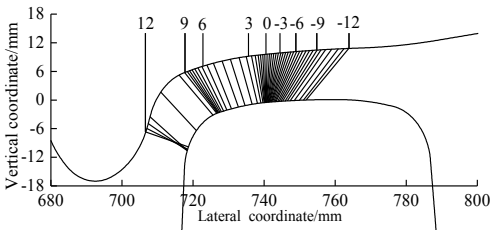

Fig.7(a) LM wheel-rail contact geometry

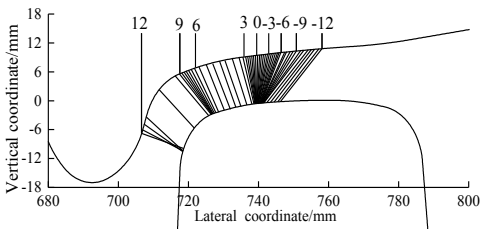

Fig.7(b) Des1 wheel-rail contact geometry

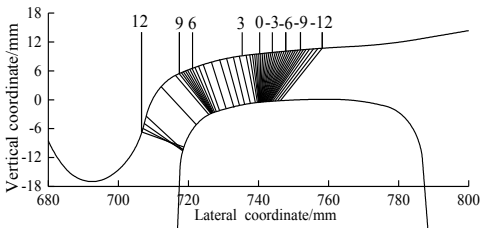

Fig.7(c) Des2 wheel-rail contact geometry

Fig.8 shows the equivalent conicity of Des1, Des2, and LM profiles. The average equivalent conicity of the three profiles at 3mm before the lateral shift of the wheelset are 0.1075, 0.104, and 0.102 respectively. The optimized profile Des1 and Des2 is closer to the optimal equivalent conicity of 0.107 for the simulated vehicle obtained in Chapter 1 and is more suitable for the simulated vehicle. It can also be seen that the equivalent conicity of the Des1 profile is slightly larger than LM when the amount of lateral movement is 6-9mm, and the equivalent conicity of the Des2 profile is significantly greater than LM. A larger equivalent conicity helps to improve the curve passing performance of the train and it can better exert the creep guiding ability between the wheel and rail.

Fig.9 shows the comparison of the rolling radius difference within 10mm of the wheelset lateral movement. It can be seen that the optimized profile increases the rolling radius difference within the range of 5-9.5mm for the wheelset lateral movement. It can be found that it is similar to the equivalent conicity. Conclusion The increase of rolling radius difference helps to improve the curve passing performance of the train and can better exert the sliding guiding ability between the wheel and the rail.

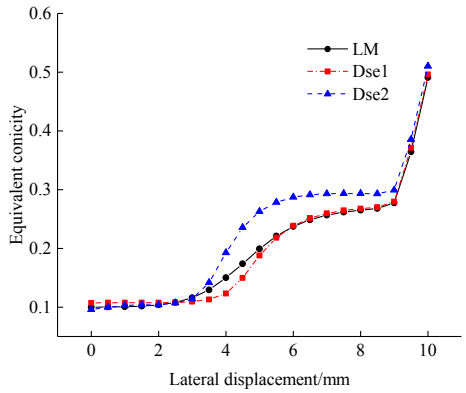

Fig.8 Comparison of equivalent conicity

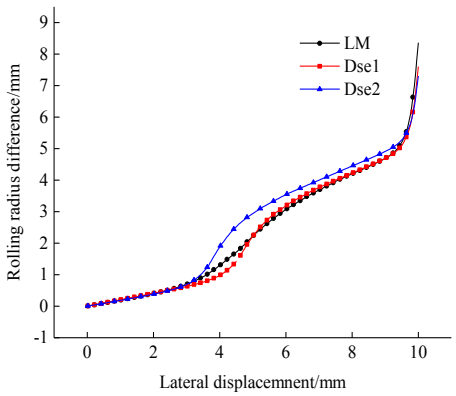

Fig.9 Comparison of rolling radius difference

5.3 Dynamic behavior on the tangent line

Use the critical hunting speed calculation method in Chapter 3 to calculate the hunting critical velocities of the three types of surfaces. The critical hunting speed of Des1, Des2, and LM profiles are 142km/h, 140km/h, and 135km/h respectively. After investigation, the bogie structure speed of this type of freight train is 120 km/h. The optimized profile is to a certain extent, the critical speed of serpentine instability of the train is increased, and all of them meet the operating requirements of 90km/h.

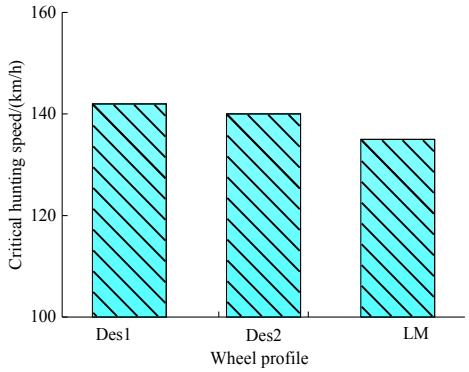

Fig.10 Critical hunting speed of three types of tread

Carry out linear running simulation calculation, set the American pentad spectrum as the line irregularity excitation, set the length of the linear line to 600 m, the sampling frequency of 200 Hz, and the passing speed of 90 km/h. Wheelset lateral vibration acceleration is an important evaluation index for train stability. UIC518 stipulates the criterion for determining the root mean square value of wheelset lateral acceleration as: $s\ddot{y}\big|_{\lim} = 5(m/s^2)$, and the $\ddot{y}$ calculation formula for acceleration root mean square is:

$$\ddot{y} = (\ddot{y}_1^{\,2} + \ddot{y}_2^{\,2} + \cdots + \ddot{y}_n^{\,2})^{0.5} \tag{29}$$

In the formula: $\ddot{y}_1, \ddot{y}_2, \cdots \ddot{y}_n$ is the lateral vibration acceleration value of the wheelset at each sampling point in the test section, and $\ddot{y}$ is the root mean square value of the lateral vibration acceleration of the wheelset in the sampling section.

According to the above formula, the root-mean-square values of the lateral vibration acceleration of the wheelset under the working condition of 90km/h are calculated as shown in Fig. 11. Among them, the maximum root means square of the LM profile is 2.96m/s^2, and the maximum root means square of the Des1 profile is 2.40m/s^2, and the maximum value of the Des2 profile is 2.42m/s^2. Two optimized types Compared with the LM profile, the maximum RMS value of the lateral vibration acceleration of the face wheel pair is reduced by 18% and 17% respectively.

According to GB/T 5599-2019 [25], the lateral stability evaluation index of freight car bogies, the obtained lateral vibration acceleration data of the side frame is subjected to 0.5~10 Hz band-pass filtering, and the result is shown in Fig.12; Evaluate whether the filtered bogie lateral vibration acceleration waveform exceeds 8 m/s^2 for 6 consecutive times, and the lateral acceleration value of the side frame when the three profiles are 90km/h running in a straight line does not exceed 8m/s^2, Des1, Des2 profiles Compared with LM, the maximum acceleration value is reduced by 10% and 8% to meet the requirements of safe operation.

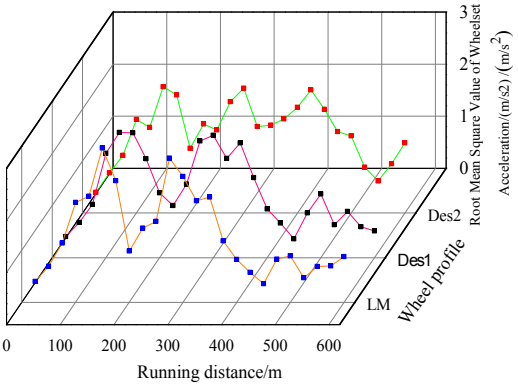

Fig.11 RMS value of lateral acceleration

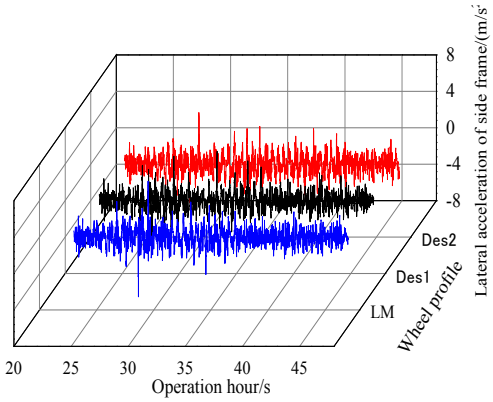

Fig.12 Lateral acceleration of bogie

The train stability index specified in my country GB/T 5599-2019 is used to evaluate the vehicle stability. The formula is:

$$W=3.57\sqrt[10]{A^3F(f)/f} \tag{30}$$

In the formula: W is the stability index, A is the lateral vibration acceleration of the vehicle body (m/s^2), f is the vibration frequency, and $F(f)$ is the weighting coefficient related to the vibration frequency f.

When calculating the vehicle stability index, first perform FFT transformation on the vehicle system acceleration response (time-domain) to obtain the acceleration frequency response function, and then calculate the respective stability index of each frequency band, and finally obtain the total frequency of the whole frequency band by formula (31) stationarity index:

$$W_{tot}=(W_1^{10}+W_2^{10}+\cdots W_n^{10})^{0.1} \tag{31}$$

The stationarity index values of the three types of surfaces are shown in Fig.13. The stationarity indicators of the three types of surfaces are 1.27, 1.19, and 1.25, respectively.

This is because the lateral vibration acceleration of the three types of wheels is not much different when running in a straight line. When the vibration is transmitted from the wheelset to the vehicle body, it is buffered and damped, and when it is transmitted to the vehicle body, the difference is further reduced.

The smoothness index of the three shapes is not higher than 3.5, and the running quality of the freight train that meets the requirements of GB/T 5599-2019 is excellent.

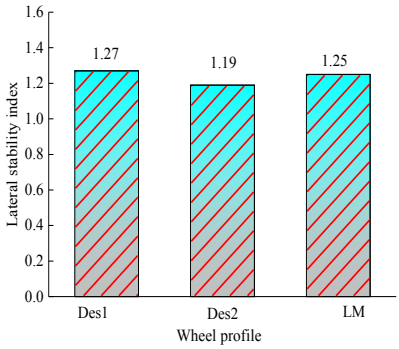

Fig.13 Lateral stability index

5.4 Curving passing performance

The American five-level spectrum is applied as the line random irregularity excitation, and the simulation parameters shown in Table 2 are used to verify the passing performance of the training curve. Process the obtained data following the data processing methods for operational stability and operational quality specified in GB/T5599-2019. Fig.14 shows the lateral force of the axle when the train passes through the R800 curve at 90km/h. The lateral forces of Des1 and Des2 are reduced compared with the LM profile. The maximum values of the lateral forces are 17% and 16% respectively. Because the two optimized profiles have a larger rolling radius difference under the same wheelset lateral displacement, the wheel-rail lateral force is reduced when crossing the curve and the derailment coefficient of the vehicle is reduced. The maximum value of the Des1 profile derailment coefficient is approximately lower than that of LM. 7%, the maximum derailment coefficient of the Des2 profile is 8% lower than that of the LM profile (Fig. 15).

The wheel load reduction rate is used to evaluate whether the train will overturn due to one wheel load reduction during train operation. The safety limit specified in GB/T5599-2019 is $(\Delta P/P)\le 0.65$, ΔP is the wheel load reduction, and P is the average net wheel weight of the axle. Fig.16 shows the schematic diagram of the wheel load reduction rate when the vehicle is assembled with three profiles at 90km/h and passes through the curve. From the Fig., it can be seen that the wheel load reduction rates of the three profiles have similar changes. The wheel load reduction rate is on the curve. The maximum difference of the maximum rate is 3%, and the maximum wheel load reduction rate of the three types of profiles is less than 0.65 when passing through the curve, which is in line with the safe operation regulations.

The lateral acceleration of the bogie when the train passes through the curve at 90 km/h is subjected to 0.5~10 Hz band-pass filtering. The lateral acceleration of the bogie is shown in Fig. 17. The lateral acceleration of the three types of profiles changes almost the same during operation. None of the bogies was unstable.

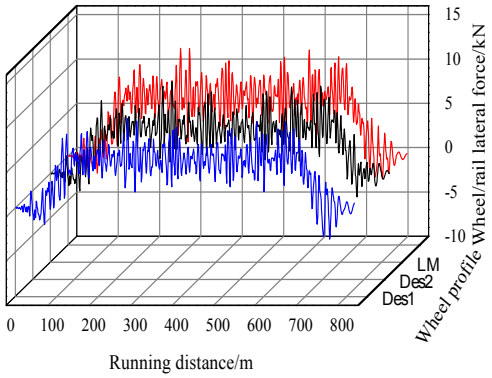

Fig.14 Lateral force of wheel-rail

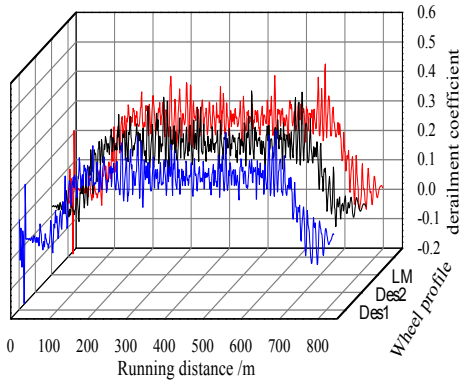

Fig.15 Derailment coefficient

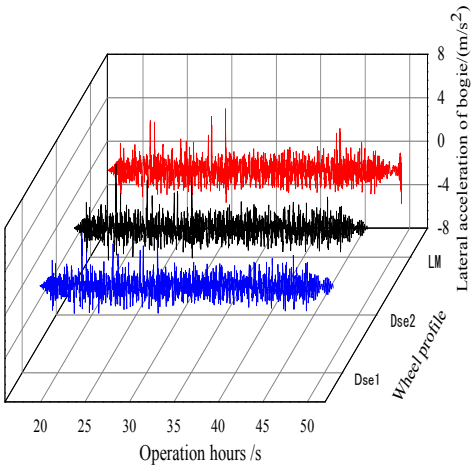

Fig.16 Rate of wheel load reduction

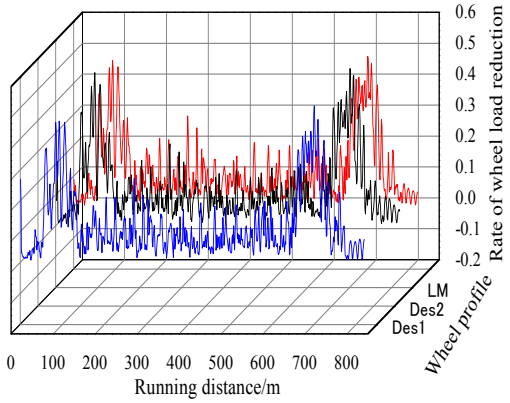

Fig.17 Lateral acceleration of bogie

The wear index is used to evaluate the wear performance of the wheel and rail, and its calculation formula is as follows:

$$We = F_x\xi_x + F_y\xi_y \tag{32}$$

In the formula, We is the wear index of the wheel and the rail at a certain time, F_x and F_y are the longitudinal and lateral creep forces of the wheel and the rail respectively; ξ_x and ξ_y are the longitudinal and lateral creep rates of the wheel and the rail respectively.

The wheel-rail wear index of the three types of profiles passing through the curve at 90km/h is shown in Fig.19. Compared with the LM profile, the average wear index of the Des1 profile and Des2 profile on the curve decreases by 5% and 2%. After the profile optimization, the dynamic performance of the training curve is improved, the creep state of the train is improved, and the wear index of the left and right wheel and rail is reduced.

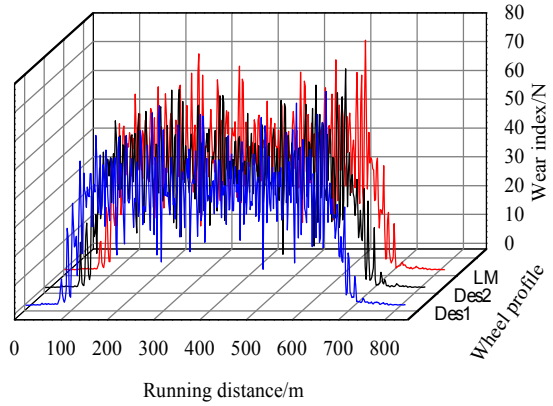

Fig.19 Wear index

6 Conclusion

The vehicle dynamics model was established based on the actual parameters and track conditions of the operating actual vehicles, and the matching performance of the equivalent conicity with the vehicle and track was analyzed, and the optimal equivalent conicity of the simulated vehicle was determined to be 0.107. The wheel profile curve is geometrically deduced, the arc parameters of the wheel profile are used as design variables, and the comprehensive objective function of the train dynamics performance index is used to establish the optimal design model of the wheel profile.

The wheel-rail contact characteristics of the optimized profile are analyzed, and the equivalent conicity of the

optimized profile is closer to the best equivalent conicity of the simulated vehicle, which ensures serpentine stability during straight-line running. Between the 6-9mm wheelset lateral displacement, the equivalent conicity and wheel diameter difference of the two optimized profiles are larger than that of the LM profile, which enables the vehicle to have a larger rolling radius difference when running in a curve, and improves the curve passing performance. Comparing and analyzing the dynamic performance of the two optimized profiles and the LM profile, it is found that when running in a straight line: the RMS value of the wheelset acceleration of the two optimized profiles is effectively reduced, the nonlinear critical speed is slightly increased, and the bogie is laterally stable. The performance and vehicle stability indicators have been improved. When the curve is running, the wheel-rail lateral force is significantly reduced, the derailment coefficient, wheel load reduction rate and wear index are reduced, and the vehicle dynamics of the optimized profile are improved to meet the speed-up operation of freight trains.

Acknowledgement: The present work was supported by Sichuan Science and Technology Program (2020YJ0308 and 2021YJ0026).

Reference

[1] China broadcasting corporation. ["Thirteenth Five-Year" Achievement Tour] the turnover of railway freight volume ranks first in the world, 2021-01-17.

[2] Jin X, Liu Q. Tribology of wheel and rail, 2004.

[3] Wang C, Luo S, Wu P, et al. Effect of hollow worn tread on dynamic performance of high-speed electric multiple units: 1-8.

[4] Jin X, Zhao G, Liang S, et al. Characteristics mechanisms influences and counter measures of high speed wheel/rail wear, 2018, 54(04): 3-13.

[5] Wu H. Investigation of wheel/rail interaction on wheel flange climb derailment and wheel/rail profile compatibility, 2000.

[6] Cui D, Li L. Wheel-rail profiles matching design considering railway track parameters, 2010(4): 410-417.

[7] Cui D, Li L, Jin X, et al. Numerical optimization technique for wheel profile considering the normal gap of the wheel and rail, 2009, 45(12): 205-211.

[8] Shen G, Ye Z. Unique design method for wheel profile considering contact angle function, 2002, 30 (9): 1095-1098.

[9] Ye Z, Shen G. Design of independently rotating wheel tread shape, 2003,41 (1): 19-21.

[10] Shevtsov I Y, Markine V L, Esveld C. Optimal design of wheel profile for railway vehicles, 2005(258): 1002-1030.

[11] Jahed, Farshi, Eshraghi, Nasr. A numerical optimization technique for design of wheel profiles, 2008, Vol.264. No.1-2: 1-10.

[12] Liu Y. Study on contact geometry and geometric profile optimization of high-speed wheel-rail, 1999.

[13] Cheng D, Wang C, Liu J, et al. Research on the mathematical model for wheel profile optimization with arc parameters as design variables, 2011,32(6): 107-113.

[14] Polach O. Wheel profile design for target conicity and wide tread wear spreading, 2011, 271: 195–202.

[15] Lian S, Li J, Yang W. Analysis of track irregularity spectrum of Shanghai-Kunming and Jinhua-Wenzhou railways, 2010,38(02): 257-262.

[16] Zhou S, Tao Y, Zhang Z. SIMPACK 9 Example Tutorial (Part 2), 2013.

[17] Miao B, Simpack Dynamic Analysis Advanced Tutorial, 2010.

[18] Zhang J. Optimal design research of railway vehicle wheel profile, 2012.

[19] Chen Z, Wang C. Railway vehicle dynamics and control, 2004.

[20] Ministry of railways of the people's republic of China. TB/T 449-1976 Wheel profile for locomotive and vehicle, 1976.

[21] Oldrich Polach, A. Vetter. methods for running stability prediction and their sensitivity to wheel/rail contact geometry. Extended abstracts of the 6th international conference on railway bogies and running gears, Budapest, September 2004: 62-64.

[22] Cui D, Li L, Jin X, et al. Influence of vehicle parameters on critical hunting speed based on Ruzicka model, 2012, 25(03): 536-542.

[23] Yu L. MATLAB intelligent algorithm 30 case analysis, 2015.

[24] Lei Y, Zhang S. MATLAB genetic algorithm toolbox and application, 2014.

[25] Standardization Administration. GB/T 5599-2019 Specification for dynamic performance assessment and testing verification of rolling stock, 2019.